Journal of Alloys and Compounds 509 (2011) 1294–1300

Contents lists available at ScienceDirect

Journal of Alloys and Compounds

journal homepage: www.elsevier.com/locate/jallcom

Effect of ammoniating temperature on microstructure and optical properties of one-dimensional GaN nanowires doped with magnesium

Feng Shi*, Dongdong Zhang, Chengshan Xue

College of Physics & Electronics, Shandong Normal University, Jinan, 250014, PR China

ARTICLE INFO

Article history:
Received 3 September 2010
Received in revised form 1 October 2010
Accepted 6 October 2010
Available online 14 October 2010

Keywords:
Mg-doped GaN nanowires
Ammoniating temperature
Microstructure
Optical properties

ABSTRACT

One-dimensional GaN nanowires doped with Mg element have been successfully prepared on Si (1 1 1) substrates by magnetron sputtering through ammoniating Ga_2O_3/Mg thin films, and the effect of the ammoniating temperatures on the microstructure and optical properties of the GaN nanowires was investigated in detail. X-ray diffraction (XRD), X-ray photoelectron spectroscope (XPS), FT-IR spectrophotometer, Scanning electron microscope (SEM), high-resolution transmission electron microscope (TEM), and photoluminescence (PL) spectrum were carried out to characterize the microstructure, morphology, and optical properties of GaN nanowires. The results demonstrate that ammoniating temperature has a significant effect on microstructure, morphology and optical properties of GaN nanowires. GaN nanowires after ammoniation at 900 °C for 15 min are straight, smooth and of uniform thickness along spindle direction with the highest crystalline quality. The growth direction of these nanowires is parallel to [1 0 0] orientation.

1. Introduction

One-dimensional GaN nanostructures are promising in the field of full-color panel displays and nanometer electronic devices with high electron migration rate [1–3]. Compared with other methods [4–7], p-type doping and p–n junctions are of very interest for the fabrication of nanostructures [1,2]. The formation of p-typed GaN films is the key technology in developing these devices. According to our previous experimental results, the intermediate layer between Si substrates and Ga_2O_3 had great influence on the modality and characteristics of the GaN nanowires. p doping of GaN nanowires with Mg as dopant is more effective in practice than with other dopants, because the ionic radii of Mg (0.65 Å) is only slightly greater than that of Ga (0.62 Å), and the gallium positions can be easily substituted by Mg under certain conditions. In this article, high-quality Mg-doped GaN nanowires have been fabricated on Si (1 1 1) substrates through ammoniating Ga_2O_3 films doped with Mg element at different temperatures for 15 min. The effect of ammoniating temperatures on microstructure, morphology and optical properties are studied in detail as a progress report of the results published previously in the other papers [8–10].

2. Experimental procedures

Mg-doped GaN nanowires have been fabricated through ammoniating Ga_2O_3 films doped with Mg under flowing ammonia atmosphere. First, the Mg-doped Ga_2O_3 films were deposited on Si (1 1 1) substrates by sputtering the Mg target of 99.99% purity and the sintered Ga_2O_3 target of 99.999% purity in a JCK-500A radio frequency magnetron sputtering system. Both the Mg target and Ga_2O_3 target were subjected to direct-current (DC) and radio-frequency (RF) magnetron sputtering, respectively. Next, 25–30 cycles of this process were performed for a total deposition time of about 100 min, after which the total thickness of the Mg-doped Ga_2O_3 films was about 600–900 nm. In a single sputtering cycle, first an undoped Ga_2O_3 layer of suitable thickness was deposited, followed by an approximately 5 nm Mg buffer layer deposited. Second, the Ga_2O_3 thin films as-deposited were ammoniated in a conventional tube furnace at different temperature for 15 min.The working conditions were as follows: 150 W of the RF sputtering power; 13.56 MHz of the frequency; 20 W of the DC sputtering power; 0.9×10^{-3} Pa of the background pressure; The working gas was pure Ar (≥99.99%) and the working pressure was 2 Pa.

The microstructure, composition, morphology and optical properties of the samples were studied using X-ray diffraction (XRD, Rigaku D/max-rB, Cu Kα, λ = 1.54178 Å), FT-IR spectrophotometer with Mg X-ray source (FTIR, Bruker TENSOR27), X-ray photoelectron spectroscope (XPS, Microlab MKII), scanning electron microscope (SEM, Hitachi S-570), high-resolution transmission electron microscope (HRTEM, Philips TECNAI-20), and photoluminescence spectrum (PL, LS50-fluorescence spectrophotometer).

3. Results and discussion

3.1. Microstructure and components analysis

Fig. 1 shows the X-ray diffraction patterns of the samples grown at different temperatures for 15 min.

As seen in Fig. 1, compared with JCPDS cards and other reference [11], the main phase is hexagonal wurtzite GaN with lattice constant $a = 0.3186$ nm and $c = 0.5178$ nm, with the diffraction peaks located at $2\theta = 32.1°$, 34.2° and 36.4° corresponding to (1 0 0), (0 0 2) and (1 0 1) planes. No peak of Ga_2O_3, Mg or MgO is observed, indi-

* Corresponding author. Tel.: +86 531 86282521; fax: +86 531 86282521.
E-mail address: sf751106@sina.com.cn (F. Shi).

0925-8388/$ – see front matter © 2010 Elsevier B.V. All rights reserved.
doi:10.1016/j.jallcom.2010.10.017

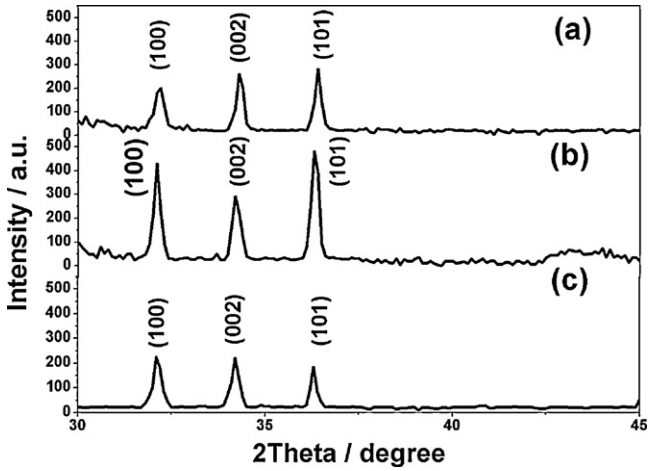

Fig. 1. X-ray diffraction patterns of samples at different temperatures for 15 min. (a) 850 °C; (b) 900 °C; (c) 950 °C.

cating that neither Ga_2O_3, Mg metal nor MgO coats the sample surface. Meanwhile, there is a small blue-shift comparing those samples without magnesium-doping. The intensity of GaN at 900 °C is stronger than that of samples synthesized at 850 °C and 950 °C, so crystallinity of GaN is at its highest. The diffraction peak intensities decrease When ammoniating temperature is lower or higher than 900 °C, which is probably caused by incomplete reaction at lower temperature and decomposition or sublimation at higher temperature [12].

To further analyze components of the GaN samples, FT-IR test was carried out for the sample after ammoniation at different temperatures for 15 min, as shown in Fig. 2.

As seen in Fig. 2, there are three well-defined prominent absorption bands, located at 561 cm^{-1} of the sample (b) (563 cm^{-1} of the sample (a), 566 cm^{-1} of the sample (c)), 609 cm^{-1}, and 1101 cm^{-1}. The band at 561 cm^{-1}, 563 cm^{-1} or 566 cm^{-1} corresponds to Ga–N stretching vibration in hexagonal type GaN crystal [13,14], and the other bands correlate to the Si substrate. The peak at 609 cm^{-1} is associated with the local vibration of substituted carbon in the Si crystal lattice [15], whereas the band at 1101 cm^{-1} is attributed to the Si–O–Si asymmetric stretching vibration because of the oxygenation of the Si substrate [16]. There is no Ga–O bond or other absorption band in the spectrum [17], therefore, Ga_2O_3 films react with NH_3 completely and form hexagonal type GaN crystal, which is the same as the results of the XRD. With the variation of temperature, the intensities and locations of absorption bands located at 609 cm^{-1} and 1101 cm^{-1} do not change accordingly. However, there are obvious changes for the absorption bands corresponding to Ga–N bond with the increase of ammoniating temperature, which is closely related with the amount of grains in the GaN films at different temperatures. The presence of Ga–N stretching vibration absorption bands prove that the samples are GaN compounds.

The sample ammoniating at 900 °C for 15 min was also characterized by XPS [10] as shown in Fig. 3

The binding energy of N1s is 397.6 eV, observed from Fig. 3. The percentage of elements is calculated according to the formula [18] as follows.

$$X\% = \frac{A_x/S_x}{\sum_{i=1}^{N} A_i/S_i}$$

A_x (A_i) indicates the peak area of element, $x(i)$; S_x (S_i) is the atomic sensitivity factor of $x(i)$ element; N is the number of total elements. The values of the atomic sensitivity factor of Ga and N atomics are 6.9 and 0.38, respectively. Therefore, quantification of peaks shows that the atomic ratio of Ga to N is approximately 1:1.09.

Fig. 3(a) shows the XPS images of N1s, Ga2p, Ga3d, and O1s for GaN synthesized at the ammoniating temperature of 900 °C, respectively. Fig. 3(a) shows the general scan in the binding energy ranging from 0 eV to 1100 eV with the main components being Ga, C, N, and O with XPS peaks at the location of Ga3d (20.1 eV), Ga3p (109.1 eV), Ga3s (167.3 eV), C1s (288.3 eV), N1s (397.6 eV) and O1s (534.3 eV). The strong peak at the site of 189.6 eV is LMM Auger peak of Ga element. C and O arise from the surface pollution of the sample [19]. As observed, the energy peak for N1s shown in Fig. 3(b) is centered at 397.6 eV, instead of 399 eV (binding energy of N element existing as atomic style), similar to the results of Li (397.4 eV) [20] and Veal (397.6 eV) [21], i.e., the N atom exists as a nitride. The width and slight asymmetry of the N1s peak are attributed to N–H_2 and N–H_3 formation due to the interaction between N_2 and NH_3 at the GaN film surface [22]. As seen in Fig. 3(c), the core level of Ga has a positive shift from elemental Ga. This shift in the binding energies of Ga and N confirms the bonding between Ga and N and the absence of elemental gallium. The binding energies of $Ga2p_{3/2}$ and $Ga2p_{1/2}$ are 1145.0 eV and 1118.1 eV respectively, which are consistent with the results reported by different reference of $Ga2p_{1/2}$ (1117.4 eV) [23], $Ga2p_{3/2}$ (1144.8 eV) [24], and $Ga2p_{3/2}$ (1144.3 eV) [25]. No bond formation is observed between Ga and O as the Ga3d spectrum does not show any satellite peak corresponding to β-Ga [25], shows the Ga atom existing only as combined GaN, not Ga_2O_3. As shown in Fig. 3(d), the O1s peak is centered at 530.9 eV. According to Amanullah et al. [26], generally, the O1s peak had been observed in the binding energy region of 529–535 eV, and the peak around 529–530 eV is ascribed to lattice oxygen [27]. For chemisorbed O_2 on the surface, the binding energy ranged from 530.0 eV to 530.9 eV. Therefore, the O1s peak in the present work is part of chemisorbed oxygen. Fig. 3(e) indicates the peak of $Mg2P_{3/2}$

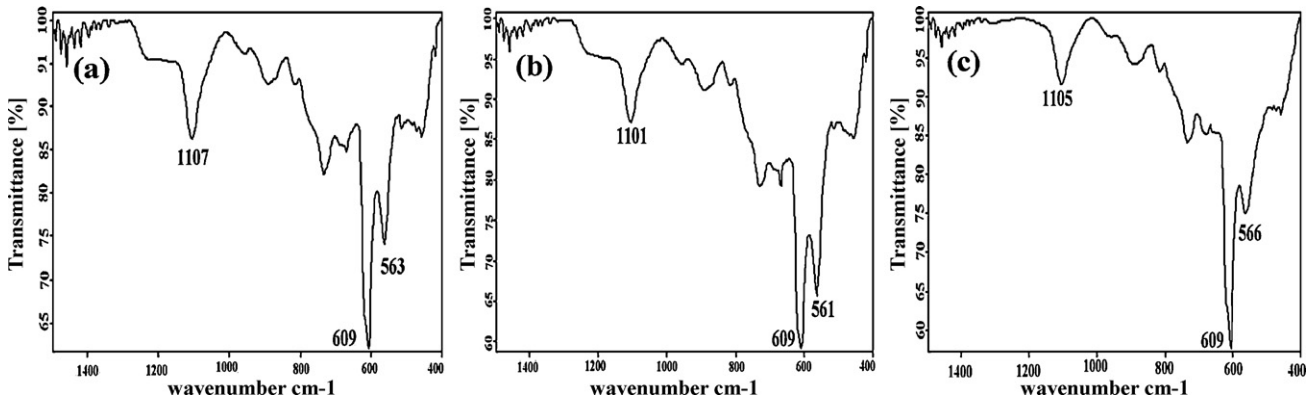

Fig. 2. FTIR patterns of the samples ammoniated at different temperatures for 15 min. (a) 850 °C; (b) 900 °C; (c) 950 °C.

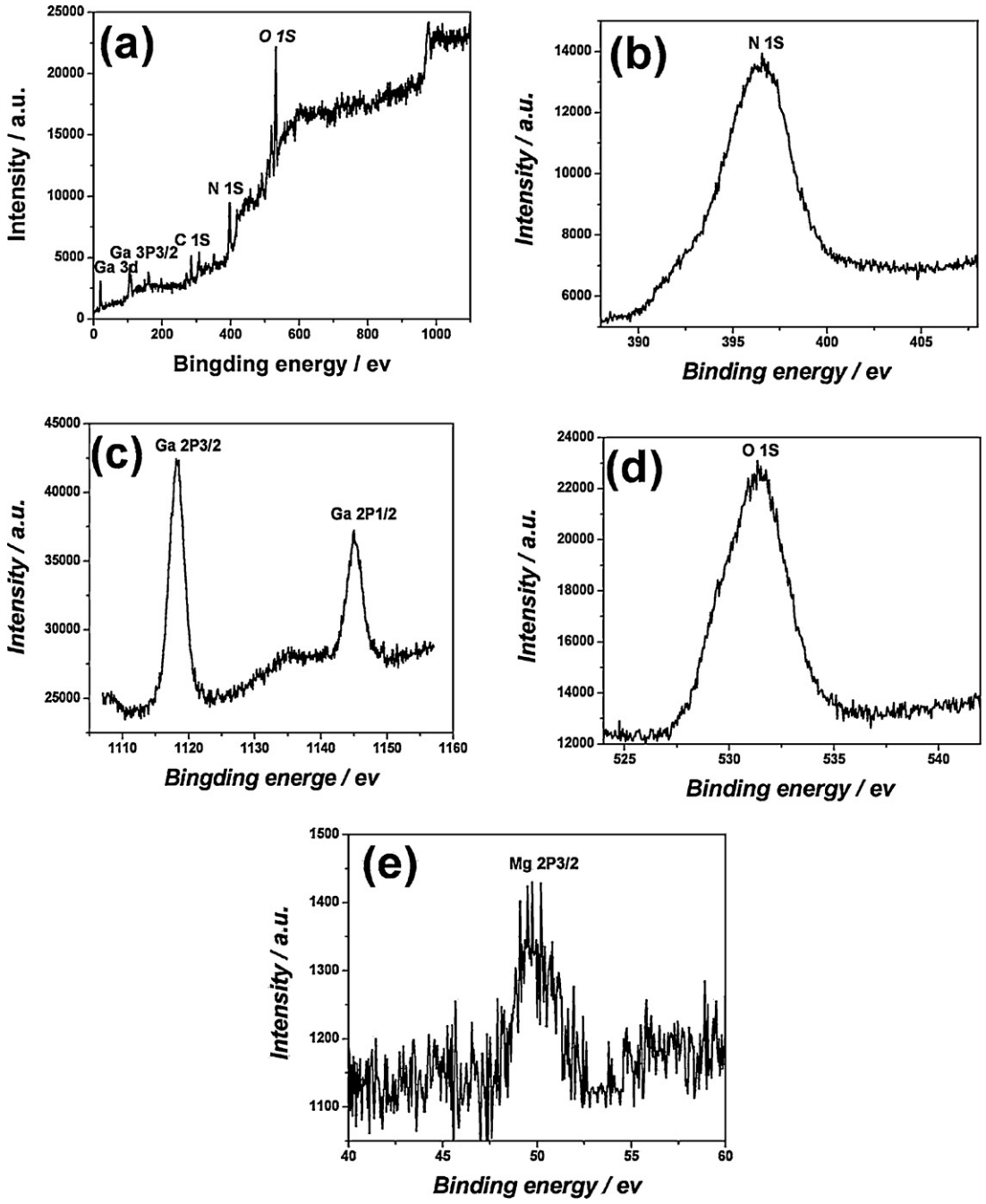

Fig. 3. XPS spectrum of the sample ammoniated at 900 °C for 15 min, (a) general scan spectrum; (b) N1s band; (c) $Ga2p_{1/2}$ and $Ga2p_{3/2}$ band; (d) O1s band; (e) $Mg2p_{3/2}$ band.

is at the site of 49.3 eV, being consistent with the bonding energy of Mg [28]. The XPS results show that the sample is Mg-doped GaN, the same as that of the XRD and FITR.

3.2. Surface morphology

Fig. 4 shows the typical SEM images of the sample grown at 850 °C.

Fig. 4 shows many cluster-like nanowires distributed on the sample surface, each of which grows radially outward, from the same point on the substrate. These nanowires are thinner in diameter but rough on the surface. The size of these nanowires is about 35 nm in diameter and 10–20 μm in length.

Fig. 5 shows the typical SEM images of the sample grown at 900 °C.

Fig. 5 shows the sample consists of a large number of one-dimensional nanowires distributed evenly on the substrate. Compared with the nanostructures in Fig. 4, these samples have cleaner surfaces and of greater quantity. Most of which are straight and smooth, of uniform thickness along the spindle direction, and interwine with each other having a thicker diameter of 50 nm and longer length of several tens of microns.

Fig. 6 shows the typical SEM images of the sample grown at 950 °C.

It can be clearly observed from Fig. 6 that there are many gossypine structures distributed on the substrate surface.

With the increase in ammoniating temperature, the diameter and length increase gradually, whereas the number of them first increases and then decreases. The quality and quantity of the sample synthesized at 900 °C is the highest and most than those of

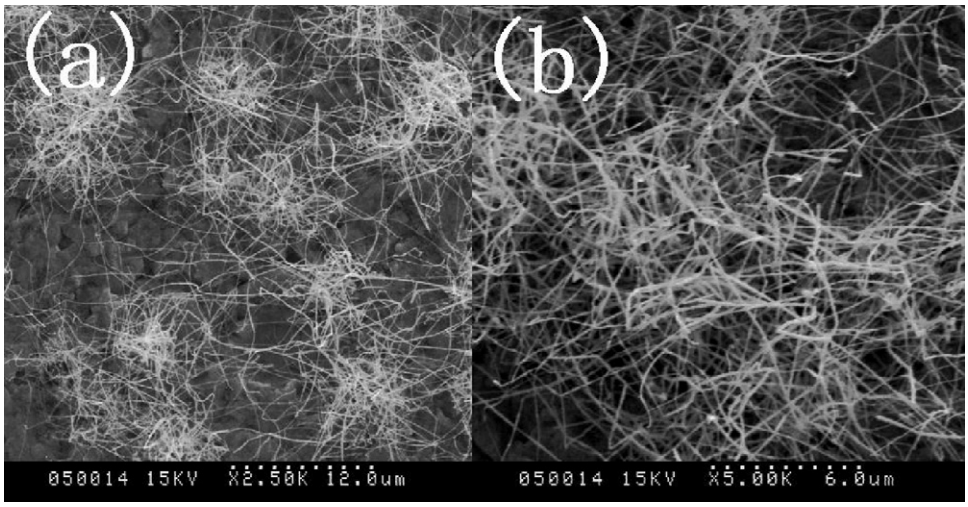

Fig. 4. SEM images of the sample grown at 850 °C. (a) 2.5 K; (b) 5 K.

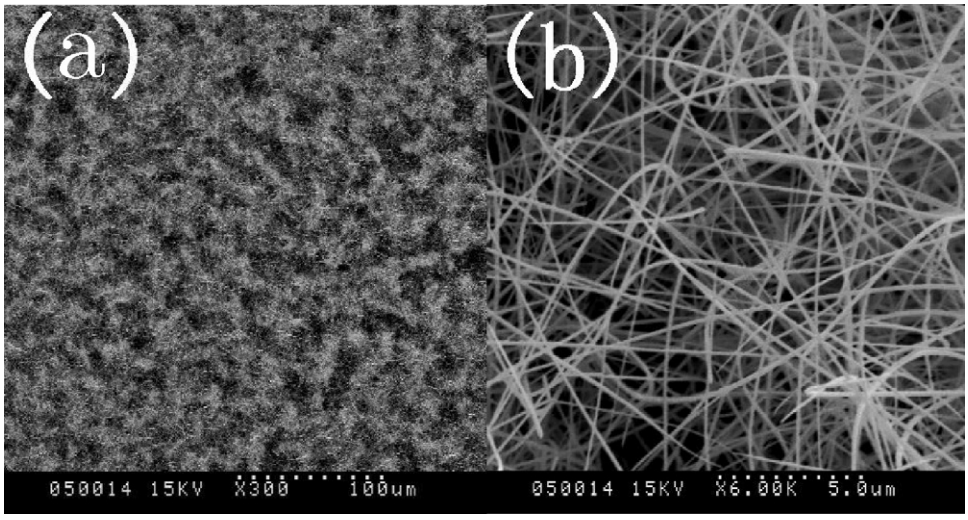

Fig. 5. SEM images of the sample grown at 900 °C. (a) 300 K; (b) 6 K.

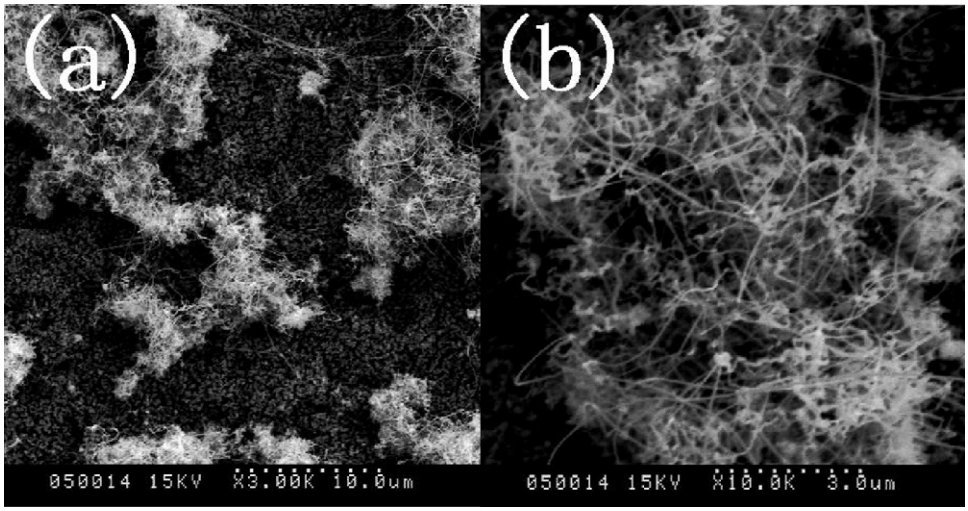

Fig. 6. SEM images of the sample grown at 950 °C, (a) 3 K; (b) 10 K.

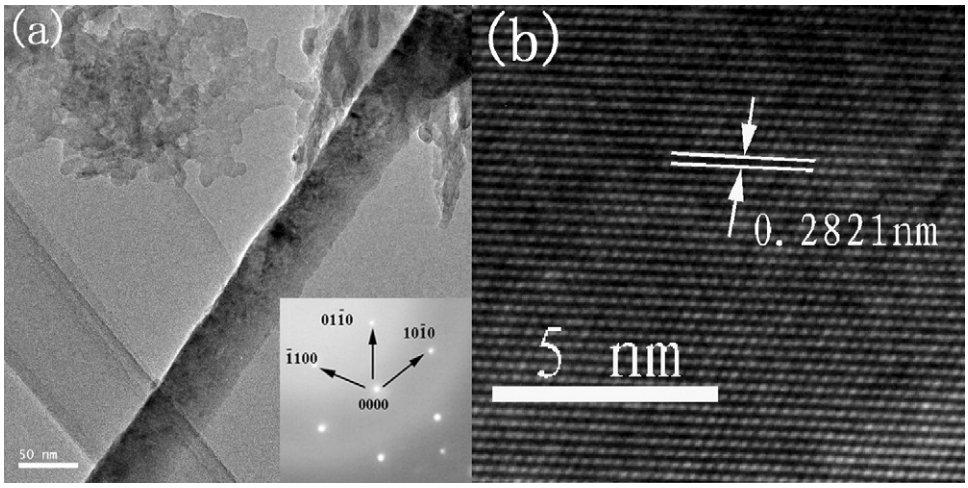

Fig. 7. TEM,SAED and HRTEM images of an individual nanowire grown at 850 °C for 15 min.

the other samples fabricated at 850 °C and 950 °C with the purest surface. This shows that the ammoniating temperature has great influence on the morphology of the GaN nanostructures.

Fig. 7 shows the TEM, SAED and HRTEM images of an individual nanowire grown at 850 °C.

Fig. 7(a) shows that the nanowire is about 35 nm in diameter with straight and smooth surface. Meanwhile, it shows the GaN nanowire is solid structure while not hollow tubular structure. Diffraction spots from SAED (the inset in Fig. 7(a)) are regular and correspond to the diffraction direction of [1 $\bar{2}$ 1 $\bar{3}$], which shows GaN nanowire is monocrystal with hexagonal wurtzite structure. The HRTEM lattice image of the straight GaN nanowire, and the well-spaced lattice fringe in the image indicate a single crystal structure of GaN nanowires with high crystalline quality. The crystal plane spacing of the nanowire is about 0.2821 nm, which is larger than that of the (1 0 0) crystal plane spacing (0.2757 nm) of hexagonal GaN single crystal [19], because of the Mg-doping slightly changing the lattice constants of the GaN, as shown in Fig. 7(b). The growth direction of this nanowire is parallel to [1 0 0] orientation.

Fig. 8 shows the TEM and HRTEM images of an individual nanowire grown at 900 °C.

Fig. 8(a) shows that the nanowire is 50 nm in diameter with straight and smooth surface and uniform thickness along spindle direction. As seen from Fig. 8(b), HRTEM lattice image of straight GaN nanowire, the well-spaced lattice fringe in the image indicate a single crystal structure of GaN nanowire with high-quality crystalline. The crystal plane spacing of nanowire is about 0.281 nm without dislocations and defects, which is larger than that of (100) crystal plane spacing (0.2757 nm) of hexagonal GaN single crystal [19]. Mg-doping also slightly changes the lattice constant of GaN.

Fig. 9 shows the TEM and HRTEM images of an individual nanowire grown at 950 °C.

Fig. 9(a) shows that the nanostructure is 75 nm in diameter with coarse surface. The reason for the coarse surface is attributed to decreased mass transportation of Ga affected by the rich-N atmosphere and Mg doping during grain growth [29]. The crystal plane spacing of nanowires is about 0.2789 nm, with many dislocations and defects shown in Fig. 9(b).

Therefore, the crystal plane spacing of the nanowire is about 0.2821 nm at 850 °C, 0.281 nm at 900 °C, and 0.2789 nm at 950 °C, i.e., decreases with the increasing temperature. In short, the temperature affects the crystal plane spacing of the nanowires, and the amount of dislocations and defects increase at higher temperature of 950 °C.

3.3. Optical properties

Fig. 10 is the photoluminescence spectrum of the samples ammoniated at different temperatures for 15 min, detected with

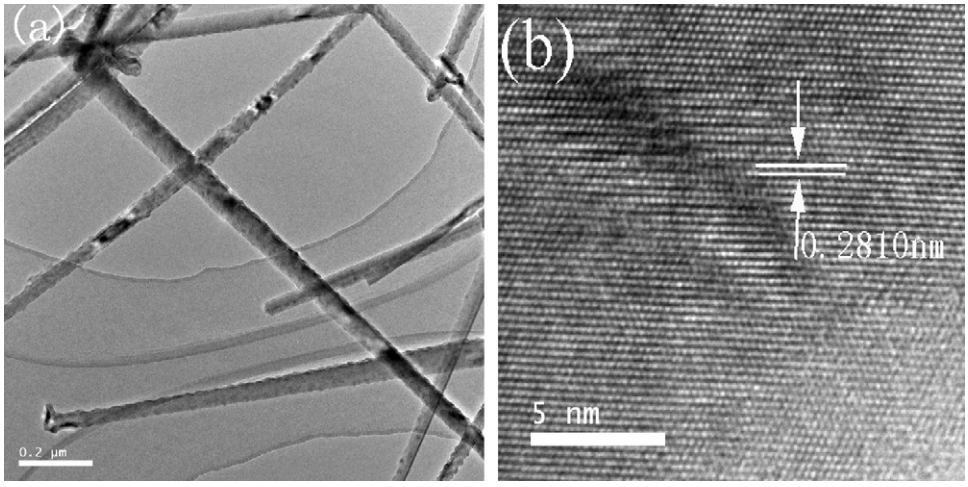

Fig. 8. TEM and HRTEM images of an individual nanowire grown at 900 °C for 15 min.

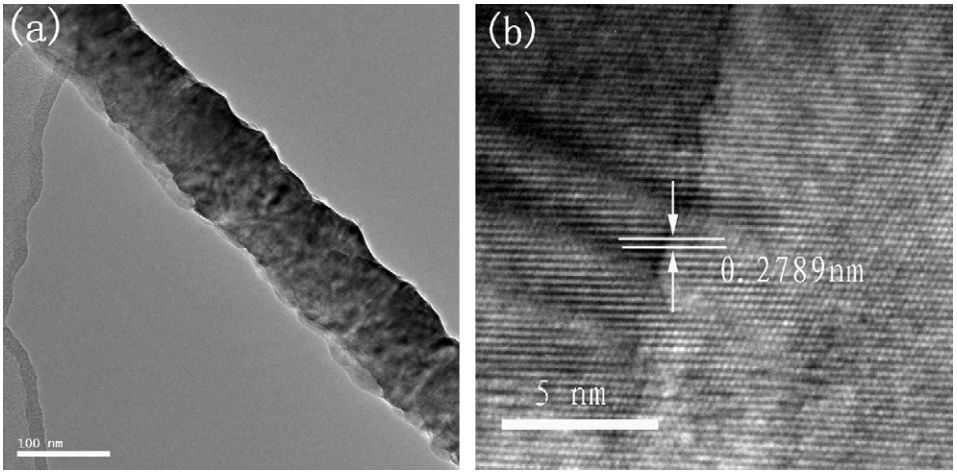

Fig. 9. TEM and HRTEM images of an individual nanowire grown at 950 °C for 15 min.

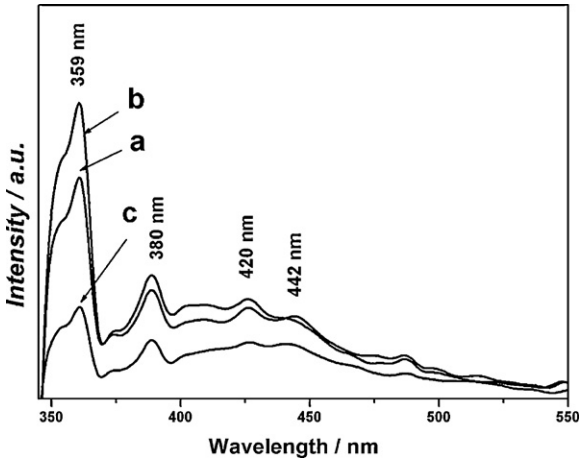

Fig. 10. Photoluminescence spectra of the samples grown at different temperatures for 15 min. (a) 850 °C; (b) 900 °C; (c) 950 °C.

He–Cd laser used as the excitation source (with a wavelength of 325 nm) at room temperature.

There are four emission peaks in Fig. 10, at 359 nm, 380 nm, 420 nm, and 442 nm, respectively. Bulk GaN shows photoluminescence at 370 nm at room temperature [19]. According to the equation $E_v = 1240/\lambda$ eV, the peak at 359 nm corresponds to $E_v = 3.45$ eV. Thus, a clear blue-shift of the band-gap emission has occurred, and this is consistent with the Burstein–Moss effect [30]. The other three peaks located at 380 nm, 420 nm and 442 nm correspond to 3.26 eV, 2.95 eV, and 2.80 eV, respectively. As for the emission peak at 380 nm, it is caused by the electrons transition from the GaN conduction band minimum to shallow acceptor level of Mg (acceptor level of Mg is at the site of 200 meV above valance band). The emission bands at the site of 420 nm and 442 nm are caused by transitions from a deep donor to the shallow Mg acceptor, which consists with the results of Zolper et al. [31]. The locations of the four emission peaks do not change but the strength of the emission peaks varies obviously with the variation in ammoniating temperature, which indicates the optical properties are closely related to ammoniating temperature. The luminous intensity of GaN nanowires is at its highest at 900 °C.

4. Conclusion

The only phase of the samples fabricated by magnetron sputtering method is the hexagonal wurtzite GaN crystal identified by XRD analysis. Growing at 900 °C for 15 min is the best condition to fabricate GaN nanowires, which has the highest crystalline quality. The presence of the Ga–N bond is established by the FTIR spectrum and the N atom exists as a nitride by XPS and quantification of peaks shows that the atomic ratio of Ga to N is approximately 1:1.09. Ammoniating temperature has great effect on the microstructure, morphology and optical properties of GaN nanowires, which are straight and smooth, of uniform thickness along spindle direction, and have the size of 50 nm in diameter and several tens of microns in length with high-quality crystalline synthesized at 900 °C for 15 min. The growth direction of this nanowire is parallel to [1 0 0] orientation. PL spectra show that GaN nanowires ammoniated at 900 °C for 15 min have excellent optical properties and have a strong emission peak at 359 nm. The optical properties of the GaN nanowires are closely related to the ammoniating temperatures because the strength of emission peaks changes with the variation of temperature while their locations do not change accordingly.

References

[1] H. Morkoc, S.N. Mohammad, Science 267 (1995) 51–55.
[2] G. Fasol, Science 272 (1996) 1751–1752.
[3] S. Nakamura, Science 281 (1998) 956–961.
[4] G.S. Cheng, S.H. Chen, X.G. Zhu, Y.Q. Mao, L.D. Zhang, Mater. Sci. Eng. A 286 (2000) 165–168.
[5] C.S. Xue, Q.Q. Wei, Z.C. Sun, Z.H. Dong, H.B. Sun, L.W. Shi, Nanotechnology 15 (2004) 724–728.
[6] W.Q. Han, S.S. Fan, Q.Q. Li, Y.D. Hu., Science 277 (1997) 1287–1289.
[7] M.Q. He, I. Minus, P.Z. Zhou, S.N. Mohammed, J.B. Halpern, R. Jacobs, W.L. Sarney, L. Salamanca-Riba, R.D. Vispute, Appl. Phys. Lett. 77 (2000) 3731–3733.
[8] D.D. Zhang, C.S. Xue, H.Z. Zhuang, H.B. Sun, Y.P. Cao, Y.L. Huang, Z.P. Zou, Y. Wang, Mater. Lett. 63 (2009) 978–981.
[9] D.D. Zhang, C.S. Xue, H.Z. Zhuang, H.B. Sun, Y.P. Cao, Y.L. Huang, Z.P. Zou, Y. Wang, Y.F. Guo, Chemphyschem 10 (2009) 571–575.
[10] F. Shi, D.D. Zhang, C.S. Xue, Mater. Sci. Eng. B 167 (2010) 80–84.
[11] P. Perlin, C. Jauberthie-Carillon, J.P. Itie, A.S. Miguel, I. Grzegory, A. Polian, Phys. Rev. B 45 (1992) 83–89.
[12] Y.G. Yang, H.L. Ma, C.S. Xue, H.Z. Zhuang, X.T. Hao, J. Ma, S.Y. Teng, Appl. Surf. Sci. 193 (2002) 254–260.
[13] B.J. Hyo, R. Carsten, H. Wilson, J. Cryst. Growth 189 (1998) 439–444.
[14] Y.J. Ai, C.S. Xue, C.W. Sun, L.L. Sun, H.Z. Zhuang, H. Li, J.H. Chen, Mater. Lett. 61 (2007) 2833–2836.
[15] Y. Sun, T. Miyasato, J. Appl. Phys. 84 (1998) 6451–6453.
[16] F. Demichelis, G. Crovini, C.F. Pirri, E. Tresso, G. Amato, U. Coscia, G. Ambrosone, P. Rava, Thin Solid Films 241 (1994) 274–277.
[17] H.D. Xiao, H.L. Ma, C.S. Xue, W.R. Hu, J. Ma, F.J. Zong, X.J. Zhang, F. Ji, Diamond Relat. Mater. 14 (2005) 1730–1734.
[18] W.F. Choi, T.Y. Song, L.S. Tan, J. Appl. Phys. 83 (1998) 4968–4973.
[19] B. Monemar, Phys. Rev. B 10 (1974) 676–681.
[20] D. Li, M. Sumiys, S. Fuke, J. Appl. Phys. 90 (2001) 4219–4223.
[21] T.D. Veal, I. Mahboob, L.F.J. Piper, C.F. McConville, H. Lu, W.J. Schaff, J. Furthmüller, F. Bechstedt, Appl. Phys. Lett. 85 (2004) 1550–1552.
[22] S.W. King, E.P. Carlson, R.J. Therrien, J. Appl. Phys. 86 (1999) 5584–5593.

[23] N. Elkashef, R.S. Srinivasa, S. Major, S.C. Sabharwal, K.P. Muthe, Thin Solid Films 333 (1998) 9–12.
[24] C.R. Kingsley, T.J. Whitaker, A.T.S. Wee, R.B. Jackman, J.S. Foord, Mater. Sci. Eng. B 29 (1995) 78–82.
[25] T. Sasaki, T. Matsuoka, J. App. Phys. 64 (1998) 4531–4535.
[26] F.M. Amanullah, K.J. Pratap, V.B. Hari, Mater. Sci. Eng. B 52 (1998) 93–97.
[27] T.J. Ghuang, C.R. Brundle, D.W. Rice, Surf. Sci. 59 (1979) 413–417.
[28] K. Ueda, H. Yamamoto, M. Naito, Phys. Rev. 88 (2002) 171–175.
[29] X.M. Cai, A.B. Djurišić, M.H. Xie, C.S. Chiu, S. Gwo, Appl. Phys. Lett. 87 (2005) 183103.
[30] S.M. Zhou, X.H. Zhang, X.M. Meng, K. Zou, X. Fan, S.K. Wu, S.T. Lee, Nanotechnology 15 (2004) 1152.
[31] J.C. Zolper, M.H. Crawford, A.J. Howard, J. Ramer, H.D. Hersee, Appl. Phys. Lett. 68 (1996) 200.